Fish and Shellfish Immunology 143 (2023) 109208

Contents lists available at ScienceDirect

Fish and Shellfish Immunology

journal homepage: www.elsevier.com/locate/fsi

Full length article

# Black carp LGP2 suppresses RIG-I mediated IFN signaling during the antiviral innate immunity

Yixuan He [a,1], Ji Liu [a,b,1], Yujia Miao [a], Meiling Liu [b], Hui Wu [a], Jun Xiao [a,*], Hao Feng [a,**]

[a] State Key Laboratory of Developmental Biology of Freshwater Fish, College of Life Science, Hunan Normal University, Changsha, 410081, China
[b] College of Chemistry and Chemical Engineering, Hunan Normal University, Changsha, 410081, China

ARTICLE INFO

*Keywords:*
Innate immunity
Black carp
Interferon
LGP2
RIG-I

ABSTRACT

Laboratory of genetics and physiology 2 (LGP2), a member of retinoic acid-inducible gene (RIG)-I-like receptors (RLRs), has been reported to play different roles in IFN signaling in both mammals and teleost fish. In our previous study, black carp (*Mylopharyngodon piceus*) LGP2 (bcLGP2) has been characterized to positively regulate melanoma differentiation-associated gene 5 (MDA5). In this study, knockdown of bcLGP2 decreased the expression of host genes, including *bcIFNb*, *bcPKR*, *bcMx1*, and *bcViperin*, and also attenuated the antiviral capability of host cells. The relationship between bcLGP2 and black carp RIG-Ib (bcRIG-Ib) has been explored. Dual-luciferase reporter assay and qRT-PCR assay indicated that bcLGP2 dampened bcRIG-Ib induced transcription of type I interferons (IFNs) and interferon-stimulated genes (ISGs), including *PKR, ISG15*, and *Viperin*. Consistently, the plaque assay identified that bcLGP2 attenuated bcRIG-Ib mediated antiviral ability against spring viremia of carp virus (SVCV). Co-immunoprecipitation assay identified the interaction between bcLGP2 and bcRIG-Ib, as well as bcLGP2 and bcRIG-Ib-CARD. And bcRIG-Ib-CARD mediated antiviral ability was also attenuated by bcLGP2. Truncation mutation analysis showed DExD/H-box Helicase domain of bcLGP2 possessed a similar inhibitory effect on bcRIG-Ib to that of bcLGP2, while the C-terminus repressor domain (CTD) presented little impact on bcRIG-Ib. Furthermore, bcLGP2 enhanced the K48-linked ubiquitination of bcRIG-Ib, promoting proteasome-dependent degradation of bcRIG-Ib. Thus, our data supported the conclusion that bcLGP2 interacted with and induced degradation of bcRIG-Ib through proteasome, leading to the dampened antiviral signaling mediated by bcRIG-Ib.

## 1. Introduction

As for the first defense directly facing diverse sorts of detrimental microorganisms existing in the surrounding environment, innate immunity initially eliminates the threats brought by infective pathogens [1]. Germline-encoded pattern-recognition receptors (PRRs) are indispensable for sensing conserved microbial structures or components, namely pathogen-associated molecular patterns (PAMPs). Being the main contributor to innate immunity, PRRs are constitutively expressed in all given types of cells, adapted to versatile pathogens. Classically, PRRs including membrane-anchored Toll-like receptors (TLRs), intracellular existing Retinoic acid-inducible gene (RIG-I)-like receptors (RLRs), NOD-like receptors (NLRs) and C-type lectin receptors (CLRs) [2]. RLR family localizes in the cytoplasm and surveils for endogenous viral RNA. Once the invasion was captured, RLRs instantaneously trigger downstream antiviral inflammatory responses to remove incursive pathogens outwards and coordinate host homeostasis [3].

RIG-I, also named DDX58, together with melanoma differentiation-associated gene 5 (MDA5) and laboratory of genetics and physiology 2 (LGP2), formed the RLR family [4]. RIG-I was known as a conserved cytosolic RNA ligand harboring protein that takes charge of identifying and responding to incursive non-self viral dsRNA with the short 5′-triphosphate end (5'ppp-dsRNA) or dsRNA synthesized by ssRNA virus, activating downstream signaling cascade to produce type I IFNs, NF-κB and other inflammatory cytokines to defend virus invasion [5]. RIG-I possesses a DExD/H-box Helicase domain, catalytically acting as an ATPase to unwind dsRNA, two copies of caspase recruitment domain (CARD), which are sequestered by internal repressor domain (RD)

* Corresponding author.
** Corresponding author.
*E-mail addresses:* xiaojun2018@hunnu.edu.cn (J. Xiao), fenghao@hunnu.edu.cn (H. Feng).
[1] These authors contributed equally to this paper.

https://doi.org/10.1016/j.fsi.2023.109208
Received 31 August 2023; Received in revised form 17 October 2023; Accepted 2 November 2023
Available online 7 November 2023

(commonly called carboxy-terminal domain, CTD) in resting stages [4,6]. RIG-I plays a crucial role in fighting against Sendai Virus (SeV) and hepatitis C Virus (HCV) [7]. RIG-I stays in an inactive conformation in the resting cells, when sensing the cellular existence of double-stranded RNA viruses, RIG-I tightly binds to endogenous short 5'ppp blunt-end dsRNA [8,9], releases the hiding two copies of CARDs from RD and takes shape massive modifications and changes to transform from autoinhibitory conformation to activating state [10]. Signal-activated RIG-I transports cascaded signal to mitochondrial antiviral signaling protein (MAVS) anchoring on mitochondrion or peroxisome. As the primary mediator of RLR signaling [11], MAVS recruits and associates proteins like IFN regulator factor IRF-3/7, and initiates phosphorylation and activation of IRF-3/7. Meanwhile, the downstream TNF-α-associated recruitment factors (TRAFs), tank-binding kinase 1 (TBK1), and the IκB kinase complex (IKK) undergo potently phosphorylation/dephosphorylation and ubiquitination changes [12,13]. At last, NF-κB undergoes nuclear translocation for initiating downstream antiviral response [14].

LGP2, commonly known as DHX58, is another key component in the RLR family. This protein lacks CARDs, which are essential for MAVS transmission but it shares a DExD/H-box Helicase in N-terminus and an RD in C-terminus [15,16]. Differing from RIG-I and MDA5, mainly executing structural rearrangements on CARDs when facing virus invasion [15,17], LGP2 still has potent affinities with endogenous dsRNAs, which makes it hard to definite its accurate facilitation in innate RLR antiviral signaling pathway. In mammals, LGP2 was initially recognized as a negative responding protein to down-regulate the type I IFN induction [18]. Recent reports showed that LGP2 cooperates with MDA5 increasing type I IFN response by enhancing MDA5 dsRNA-protein or protein-protein association [19], but it makes a restriction on RIG-I/MAVS protein interaction and subsequent activation [20]. Nevertheless, in LGP2 deficient mice, the sensitivity against VSV (identified by RIG-I), or EMCV (identified by MDA5) varies in different degrees of type I IFN production and following antiviral response [21,22]. Though *in vivo* research indicated that over-expression of LGP2 in mice still augments IFN responding but relates to a much weaker level than RIG-I/MDA5 does [23]. In lower vertebrates, it is reported that grass carp LGP2 suppresses the K63-linked ubiquitination of RIG-I/MDA5, and also inhibits the activation of IFN-β or IRF3 in the early stage of GCRV infection in CIK cells [24]. LGP2 loss-of-function zebrafish decreased IFN response in the early stage of SVCV infection but heightened in the late infectious phase [25]. *In vitro* studies declared that dual functions of LGP2 are largely relevant to over-expression dose [25]. LGP2 also plays an indispensable positive role in cell apoptosis and tumor control [26,27]. In general, LGP2 ambiguously masks its modulation on innate antiviral response, which remains a capacious field to explore.

Black carp (*Mylopharyngodon piceus*) is a typical kind of carp in China, together with other three common carps, silver carp (*Hypophthalmichthys molitrix*), grass carp (*Ctenopharyngodon idella*) and bighead carp (*Aristichthys nobilis*) collectively consist of "Four Domestic Carps". Their reproductions and yields are quite significant for every Chinese dining table. However, black carp usually encounters a mass of potential threats like grass carp reovirus (GCRV) and spring viremia of carp virus (SVCV), which are two representative RNA viruses that majorly attack carps. bcRIG-I was identified and quite characterized in our lab, though bcRIG-I has a few different features from its mammalian counterparts but in line with zebrafish RIG-I [28]: there are two spliced transcripts of RIG-I, bcRIG-Ia and bcRIG-Ib. Except for non-functional bcRIG-Ia, bcRIG-Ib has great antiviral ability against virus infection being consistent with mammalian dsRNA-activated RIG-I. Besides, bcLGP2 was also investigated in our lab. We found that bcLGP2 has similar characteristics sharing core functional domains (an N-terminal DExD/H-box Helicase domain and a C-terminal domain, CTD) with bcRIG-I/bcMDA5, but lacking CARDs as its mammalian counterparts did. bcLGP2 helps MPF and EPC cells acquire improved antiviral ability against the invasion of GCRV and SVCV [29]. In this paper, we further studied the relevance between bcRIG-Ib and bcLGP2, and probed into how bcLGP2 interacts with bcRIG-Ib and inhibits the bcRIG-Ib-mediated antiviral signaling pathway, which provides a new prospect in in-depth mechanism of RIG-I and LGP2 in teleost fish.

## 2. Materials and methods

### 2.1. Cells and plasmids

HEK293T, *Epithelioma papulosum cyprinid* (EPC) cells were kept in the lab. *Mylopharyngodon piceus fin* (MPF) cells were gained from Dr. Tiansheng Chen (College of Aquatic Sciences, Jimei University) [30]. HEK293T cells were cultured at 37 °C with 5% CO2; EPC cells were cultured at 26 °C with 5% CO2; MPF cells were cultured at 26 °C with 5% CO2. All cell lines were maintained in the Dulbecco's Modified Eagle Medium (DMEM) (Yuanpei, China) containing 10% fetal bovine serum (FBS), 2 mM glutamine, 100 U/ml penicillin and 100 μg/ml streptomycin. Transfections were performed using Polyetherimide (PEI) for HEK293T and EPC cells, and LipoMax (SUDGEN, China) for MPF cells, as previously described [31]. The lab also kept the following plasmids: pcDNA5/FRT/TO (Invitrogen, USA), pEGFP-N1(Invitrogen, USA), pcDNA5/FRT/TO-bcRIG-Ib-HA, pcDNA5/FRT/TO-bcRIG-Ib-Flag, pcDNA5/FRT/TO-Flag-bcRIG-Ib-CARD, pcDNA5/FRT/TO-HA-bcLGP2, pcDNA5/FRT/TO-Flag-bcLGP2, pcDNA5/FRT/TO-Myc-bcLGP2, pRL-TK, Luci-bcIFNa, Luci-eIFN, Luci-bcIRF3, Luci-DrIFNφ1 and Luci-DrIFNφ3 (for analyzing the activity of black carp IFNa, EPC IFN, black carp IRF3, zebrafish IFNφ1 and zebrafish IFNφ3 promoters accordingly). Additionally, pcDNA5/FRT/TO-HA-Ub, pcDNA5/FRT/TO-HA-K48O-Ub (only possesses Lys-48 of poly-ubiquitin chain), pcDNA5/FRT/TO-HA-K63O-Ub (only possesses Lys-63 of poly-ubiquitin chain) were available [29]. The recombinant expression vector pcDNA5/FRT/TO-HA-bcLGP2-Helicase, pcDNA5/FRT/TO-HA-bcLGP2-CTD, pcDNA5/FRT/TO-HA-bcLGP2-ΔHelicase, and pcDNA5/FRT/TO-HA-bcLGP2-ΔCTD were constructed by cloning the CDS or the predicted functional domain of bcLGP2 into pcDNA5/FRT/TO-HA, respectively [29]. The knockdown shRNA plasmids targeting bcLGP2 were constructed according to the reference [31]. All primer information is listed in Table 1.

### 2.2. Virus production and titration

Spring viremia of carp virus (SVCV) was kept in the lab (strain: SVCV741) with stocked concentration: $2.0 \times 10^7$ PFU/mL. The indicated MOIs of SVCV were calculated by the measured cell amount and our lab's stocked SVCV concentration. The virus was replicated in EPC cells cultured in 2% FBS medium at 26 °C and the titer was evaluated through the plaque assay as previously described [32]. Briefly, the EPC cells infected with SVCV were harvested together with supernatant media and frozen at −80 °C when the cytopathic effect (CPE) was up to 50%. After freezing and thawing three times, the titers of the virus mixture were measured by the plaque assay. The 10-fold serially diluted virus supernatant was added to EPC cells and incubated for 2 h at 26 °C. The supernatant was replaced with fresh DMEM containing 2% FBS and 0.75% methylcellulose (Sangon, China) after incubation. Plaques were counted under the microscope as the following method: EPC cells were seeded in a 24-well plate 16–20 h before infection, and three parallel group cells were set for every harvested supernatant media. About 4 days after infection, when appropriate sized plaques form, we count the number of plaques. In brief, as the 10-fold serially dilution of harvested supernatant media has been added into 24-well plates separately, we chose the wells which generated the plaque number under 20 and

**Table 1**
Primers used in the study.

| Primer name | Sequence (5′-3′) | Primer information |
|---|---|---|
| **bcLGP2 Mutants** | | |
| bcLGP2-Helicase-N-F | ACTGACGGTACCGCCACCATGACGCTGCTGAAAGAGT | HA-bcLGP2-Helicase |
| bcLGP2-Helicase-N-R | ACTGACCTCGAGTTAAGCCCGCCCACTGGCCTGC | |
| bcLGP2-CTD-N-F | ACTGACGGTACCGCCACCATGGTTCAGCTTCAGTGCAGAGG | HA-bcLGP2-CTD |
| bcLGP2-CTD-N-R | ACTGACCTCGAGTTAAAAGTCAAACTCTGTCACCT | |
| bcLGP2-ΔHelicase-N-F | ACTGACGGTACCATGCGAGCTCTGAACAGCGTC | HA- bcLGP2-ΔHelicase |
| bcLGP2-ΔHelicase-N-R | ACTGACGGATCCTCAGTCGTCTAAGTCCAG | |
| bcLGP2-ΔCTD-N-F | ACTGACGGTACCATGGAGATCACTCTTAGA | HA- bcLGP2-ΔCTD |
| bcLGP2-ΔCTD-N-R | ACTGACGGGCCCTTACTGATCAGGACTGTAGCG | |
| **qRT-PCR** | | |
| epc-actin-F | AAGGAGAAGCTCTGCTATGTGGCT | *ex vivo* qRT-PCR |
| epc-actin-R | AAGGTGGTCTCATGGATACCGCAA | |
| epc-Viperin-F | GCAAAGCGAGGGTTACGAC | |
| epc-Viperin-R | CTGCCATTACTAACGATGCTGAC | |
| epc-Mx1-F | TGGAGGAACCTGCCTTAAATAC | |
| epc-Mx1-R | GTCTTTGCTGTTGTCAGAAGATTAG | |
| epc-ISG15-F | TGATGCAAATGAGACCGTAGAT | |
| epc-ISG15-R | CAGTTGTCTGCCGTTGTAAATC | |
| epc-PKR-F | CCAACATCGTCCGCTACTACTC | |
| epc-PKR-R | GCGTGTCTCCCTCACAAAG | |
| epc-IFN-F | ATGAAAACTCAAATGTGGACGTA | |
| epc-IFN-R | GATAGTTTCCACCCATTTCCTTAA | |
| SVCV-G-F | GATGACTGGGAGTTAGATGGC | |
| SVCV-G-R | ATGAGGGATAATATCGGCTTG | |
| SVCV-M-F | CGACCGCGCCAGTATTGATGGATAC | |
| SVCV-M-R | ACAAGGCCGACCCGTCAACAGAG | |
| SVCV-N-F | GGTGCGAGTAGAAGACATCCCCG | |
| SVCV-N-R | GTAATTCCCATCATTGCCCCAGAC | |
| SVCV-P-F | AACAGGTATCGACTATGGAAGAGC | |
| SVCV-P-R | GATTCCTCTTCCCAATTGACTGTC | |
| bc-LGP2-F | ACACCTCAACCTCCTCAT | |
| bc-LGP2-R | CCCTGGGACTCATACTCT | |
| bc-actin-F | TGGGCACCGCTGCTTCCT | |
| bc-actin-R | TGTCCGTCAGGCAGCTCAT | |
| bc-IFNb-F | GACCACGTTTCCATATCTTT | |
| bc-IFNb-R | CATTTTTTCTTCATCCCACT | |
| bc-Viperin-F | CCAAAGAGCAGAAAGAGGGACC | |
| bc-Viperin-R | TCAATAGGCAAGACGAACGAGG | |
| bc-Mx1-F | GACTCCTTATGTGATGGCTTGTGG | |
| bc-Mx1-R | TGAGCGTAGGCATTAGCAC | |
| bc-PKR-F | GAGCGGACTAAAAGGACAGG | |
| bc-PKR-R | AAAATATATGAGACCCAGGG | |
| **shRNA** | | |
| shbcLGP2-1-F | CCGGGCCGCTATGTGGAGAAGAAAGCTCGAGCTTTCTTCTCCACATAGCGGC TTTTTG | bcLGP2-shRNA-1 |
| shbcLGP2-1-R | AATTCAAAAAGCCGCTATGTGGAGAAGAAAGCTCGAGCTTTCTTCTCCACATAGCGGC | |
| shbcLGP2-2-F | CCGGGGACTTATTTGGGCGTCTTGTCTCGAGACAAGACGCCCAAATAAGTCCTTTTTG | bcLGP2-shRNA-2 |
| shbcLGP2-2-R | AATTCAAAAAGGACTTATTTGGGCGTCTTGTCTCGAGACAAGACGCCCAAATAAGTCC | |
| shbcLGP2-3-F | CCGGGGATGGAACAGACTTCTTTCTCTCGAGAGAAAGAAGTCTGTTCCATCCTTTTTG | bcLGP2-shRNA-3 |
| shbcLGP2-3-R | AATTCAAAAAGGATGGAACAGACTTCTTTCTCTCGAGAGAAAGAAGTCTGTTCCATCC | |
| shbcLGP2-4-F | CCGGGGAATTCACCAATGAGTATCTCTCGAGAGATACTCATTGGTGAATTCCTTTTTG | bcLGP2-shRNA-4 |
| shbcLGP2-4-R | AATTCAAAAAGGAATTCACCAATGAGTATCTCTCGAGAGATACTCATTGGTGAATTCC | |
| shbcLGP2-5-F | CCGGGGGAGTTCAGAATCAAGATATCTCGAGATATCTTGATTCTGAACTCCCTTTTTG | bcLGP2-shRNA-5 |
| shbcLGP2-5-R | AATTCAAAAAGGGAGTTCAGAATCAAGATATCTCGAGATATCTTGATTCTGAACTCCC | |
| shbcLGP2-6-F | CCGGGGAGAAGACCTTTGAAGATTGCTCGAGCAATCTTCAAAGGTCTTCTCCTTTTTG | bcLGP2-shRNA-6 |
| shbcLGP2-6-R | AATTCAAAAAGGAGAAGACCTTTGAAGATTGCTCGAGCAATCTTCAAAGGTCTTCTCC | |

counted. The plaque numbers were multiplied by the dilution ratio ($10^1$ … $10^4$, etc.) and being manipulated through the normalized process then presented as the titer of SVCV $Log_{10}$ (PFU/mL) [33,34].

### 2.3. RNA extraction and quantitative real-time PCR

Total RNA from treated EPC/MPF cells was extracted using the RNA rapid extraction kit (Magen, China). The RNA was reverse-transcribed using reverse transcriptase (Takara, Japan). The relative mRNA levels of SVCV encoded proteins (M, N, P, G), *bcLGP2*, *bcIFNb*, *bcPKR*, *bcViperin*, *bcMx1* in SVCV-infected MPF cells, and *eIFN*, *eISG15*, e*PKR*, and e*Viperin* in SVCV-infected/uninfected EPC cells were detected using qRT-PCR. The qRT-PCR was performed using the chamQ universal SYBR q-PCR Master Mix (Vazyme, China). The amplification procedure of qRT-PCR was: 1 cycle of 95 °C/10 min; 40 cycles of 95 °C/15 s, 60 °C/1 min, followed by dissociation curve analysis (60 °C-95 °C). The threshold cycle (CT) value was examined by using the manual setting on the 7500 Real-Time PCR System and exported into a Microsoft Excel Sheet for subsequent data analysis, where the relative expression ratio of the target gene was calculated by $2^{-\Delta\Delta CT}$ method. Data were normalized by β-actin expression as the internal control. Primers used for qRT-PCR assays are described in Table 1 [35].

### 2.4. Immunoblotting

HEK293T cells were seeded in 100 mm culture dishes or 6-well plates at 37 °C and transfected with plasmids. Afterwards, transfected cells were harvested with pre-cooling PBS buffer and lysed with 1% NP 40 supplemented with a protease inhibitor for immunoblotting analyzing the expression levels of the corresponding protein. In detail, the extracts

of cells were separated by 8% or 10% SDS-PAGE and then they were transferred onto PVDF membranes for immunoblotting analysis. The transferred membrane was probed with mouse-*anti*-HA/Flag/Myc monoclonal antibody (1:5000, Abmart), or mouse-*anti*-EGFP monoclonal antibody (1:5000, Sigma) which was followed by the incubation with goat-*anti*-mouse IgG (1:30000, Abmart). The target protein was visualized using BCIP/NBT Alkaline Phosphatase Color Development Kit (Thermo, USA).

### 2.5. Dual-luciferase reporter assay

EPC cells in 24-well plates were co-transfected with described plasmids, pRL-TK and indicated different fish IFN promoters (bcIFNa-pro/eIFN-pro/DrIFNφ1-pro/DrIFNφ3-pro/bcIRF3-pro). The total amount of plasmids for each transfection was balanced with empty vectors, pcDNA5/FRT/TO. The treated EPC cells were harvested and lysed by passive lysis buffer (PLB) at 24 h post-transfection. The centrifuged supernatant was used to measure firefly luciferase and renilla luciferase (as internal control) activities according to the instructions of the manufacturer (Promega, USA).

### 2.6. Co-immunoprecipitation (Co-IP)

The transfected HEK293T cells were harvested at 48 post-transfection and lysed for co-immunoprecipitation (co-IP) assay as previously described [36]. Briefly, the whole cell lysates were incubated with protein A/G agarose beads at 4 °C for 1 h. After precleaning and concentrating the beads, the anti-Flag conjugated protein A/G agarose beads were added and incubated with the supernatant media at 4 °C for 4 h. The beads were washed five times with 1% NP 40, then added into Flag peptide (Sangon, China) into the media containing a small quantity of 1% NP 40 and Flag-conjugated beads to obtain pure eluted precipitations. The eluted immunoprecipitants were boiled in a 5 × sample buffer, and then subjected to SDS-PAGE and immunoblotting analysis as above.

### 2.7. Statistics analysis

All statistics data (qRT-PCR, dual-luciferase reporter assay, and viral titration) were analyzed by two-tailed Student's t-test. Error bars represented the standard error of the mean (+SEM) of three independent experiments. Data are representative of three independent experiments. The asterisk represents the significant difference, (*) stands for $P < 0.05$, and (**) stands for $P < 0.01$.

## 3. Results

### 3.1. Knockdown of bcLGP2 attenuated host IFN signaling

In our previous study, we observed that over-expression bcLGP2 enhanced the antiviral capability of EPC and MPF cells against SVCV and GCRV [29]. To explore the antiviral capacity in host cells with bcLGP2 knockdown, we constructed shRNA recombinant plasmids targeting bcLGP2. Knockdown efficiency was analyzed using immunoblotting (IB) and qRT-PCR assays. It is obvious that bcLGP2-shRNA-4 weakened the protein expression level of exogenous bcLGP2 mostly (Fig. 1A), and the following qRT-PCR results indicated the decreased mRNA transcriptional level of endogenous bcLGP2 (Fig. 1D) in MPF cells expressing

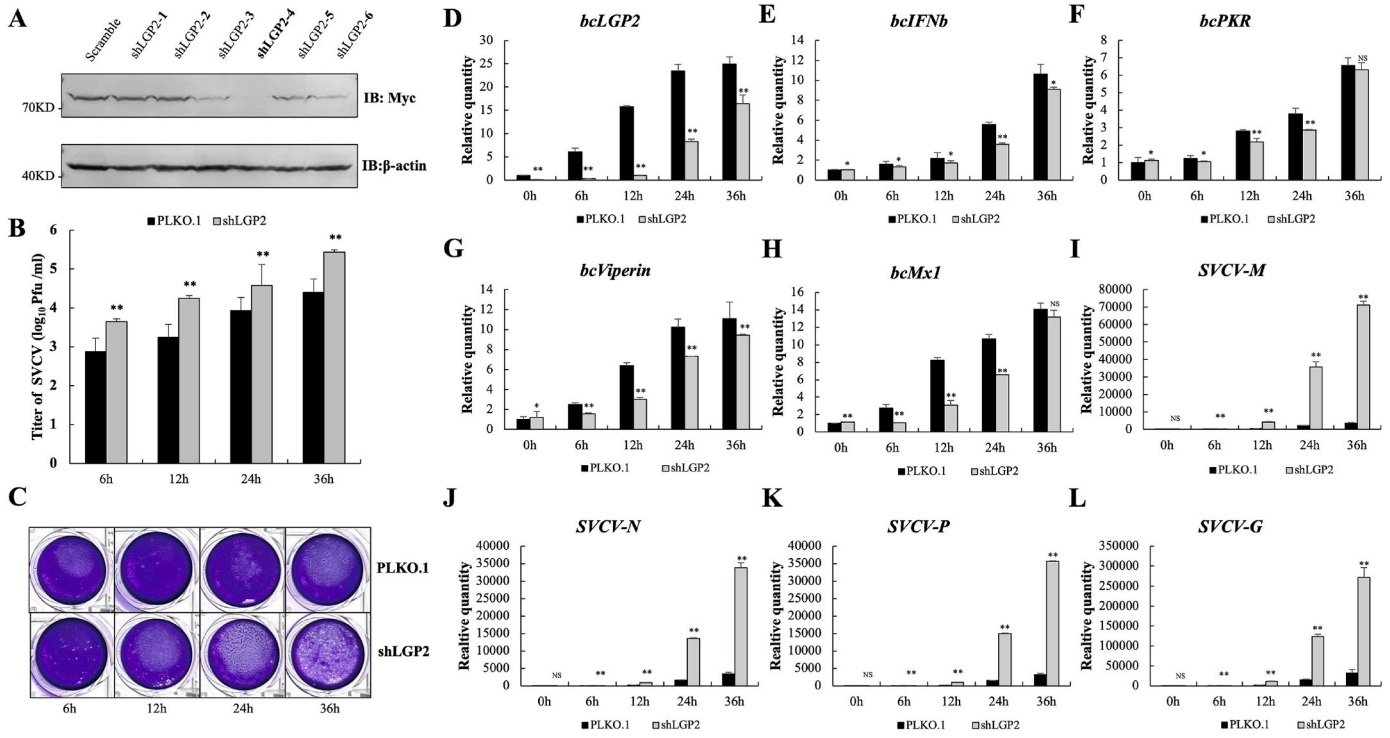


**Fig. 1.** bcLGP2 knockdown attenuated the antiviral ability of host cells. HEK293T cells co-expressing bcLGP2 and shRNA targeting bcLGP2 (shbcLGP2-1, shbcLGP2-2, shbcLGP2-3, shbcLGP2-4, shbcLGP2-5 and shbcLGP2-6) or Scramble in 6-well plates were subjected for IB assay at 48h post-transfection (A). MPF cells expressing shRNA-bcLGP2 or control (PLKO.1) in 6-well plates were infected with or without SVCV (MOI = 0.1) after 24h post-transfection for different time points (0h/6h/12/24h/36h). The collected supernatants were analyzed by viral plaque assay (B) and the cell monolayers were stained with crystal violet (C). The treated MPF cells were harvested and subjected to RNA extraction and reverse transcription to obtain cDNA and the relative mRNA levels of *bcLGP2* (D), *bcIFNb* (E), *bcPKR* (F), *bcViperin* (G), *bcMx1* (H), *SVCV-M* (I), *SVCV-N* (J), *SVCV-N* (K) and *SVCV-G* (L) were examined by qRT-PCR assays. shLGP2-1:PLKO-shRNA-bcLGP2-1; shLGP2-2: PLKO-shRNA-bcLGP2-2; shLGP2-3:PLKO-shRNA-bcLGP2-3; shLGP2-4:PLKO-shRNA-bcLGP2-4; shLGP2-5:PLKO-shRNA-bcLGP2-6; shLGP2-1:PLKO-shRNA-bcLGP2-6. Scramble: PLKO-shRNA-scramble. Error bars represent the standard error of the mean (+SEM) of three independent experiments. Data are representative of three independent experiments. *$P < 0.05$, **$P < 0.01$.

bcLGP2-shRNA-4. Thus, MPF cells expressing bcLGP2-shRNA-4 were infected with or without SVCV at indicated time points post-infection (0h/6h/12h/24h/36h) and then subjected to qRT-PCR assays. The mRNA transcriptional levels of host genes including *bcIFNb* (Fig. 1E), *bcPKR* (Fig. 1F), *bcVieprin* (Fig. 1G) and *bcMx1* (Fig. 1H) in the bcLGP2 knockdown group were significantly decreased compared with those in the control group. Moreover, plaque assay and qRT-PCR results showed that both SVCV virus titer (Fig. 1B) and mRNA transcriptional levels of SVCV encoding proteins M (Fig. 1I), N (Fig. 1J), P (Fig. 1K) and G (Fig. 1L) in the bcLGP2 knockdown group was significantly heightened compared to the control group. These results revealed that bcLGP2 enhances the host cellular antiviral capacity.

### 3.2. bcLGP2 down-regulated bcRIG-Ib mediated IFN transcription

To investigate the role of bcLGP2 in bcRIG-I-mediated IFN signaling pathway, EPC and MPF cells were transfected with plasmids expressing bcRIG-Ib and/or bcLGP2 separately, then subjected to dual-luciferase reporter assay. The results indicated that in EPC cells and MPF cells, bcLGP2 dose-dependently inhibited bcRIG-Ib-mediated transcription of bcIFNa (Fig. 2A&D), DrIFNφ3 (Fig. 2B&E) and bcIRF3 (Fig. 2C&F) promoter. Thus, the data suggested that bcLGP2 negatively regulates bcRIG-Ib-mediated IFN production.

### 3.3. bcLGP2 restricted the antiviral activity of bcRIG-Ib

We previously reported that bcRIG-Ib presents strong antiviral activity against SVCV [37]. Since bcLGP2 could dampen the IFN promoter transcription induced by bcRIG-Ib, we further investigated the impact of bcLGP2 on bcRIG-Ib-mediated antiviral ability. EPC cells were transfected with bcRIG-Ib and/or bcLGP2 plasmids and then subjected to SVCV infection through different MOIs (0.01/0.1/1) separately. The viral titer results showed that when bcRIG-Ib and bcLGP2 were co-expressed in EPC cells, the SVCV virus titer in the supernatant media was significantly increased (Fig. 3A). In addition, the cytopathic effect (CPE) in the cells co-expressing bcRIG-Ib and bcLGP2 were also much more than that in the cells expressing bcRIG-Ib alone (Fig. 3B).

To probe into the mRNA transcriptional variation of IFNs (*eIFN)* and interferon stimulated genes (*ePKR*, *eISG15*, and *eViperin*), EPC cells were co-transfected with bcRIG-Ib and/or bcLGP2, then treated with or without SVCV infection. The qRT-PCR results showed that over-expressing bcRIG-Ib alone significantly inhibited the mRNA transcriptional levels of SVCV encoding proteins M (Fig. 3C), P (Fig. 3D), G (Fig. 3E) and N (Fig. 3F), but the transcription levels of these viral genes were increased in the bcLGP2 and bcRIG-Ib co-transfection group. In addition, the mRNA levels of *eIFN* (Fig. 3I), *ePKR* (Fig. 3G), *eISG15* (Fig. 3H) and *eViperin* (Fig. 3J) induced by bcRIG-Ib were also attenuated by bcLGP2. All these data suggested that the incremental antiviral activity induced by bcRIG-Ib was notably disabled by bcLGP2.

### 3.4. Protein interaction between bcLGP2 and bcRIG-Ib

We further investigated the possible interaction between bcLGP2 and bcRIG-Ib. HEK293T cells were transfected with bcRIG-Ib and/or bcLGP2

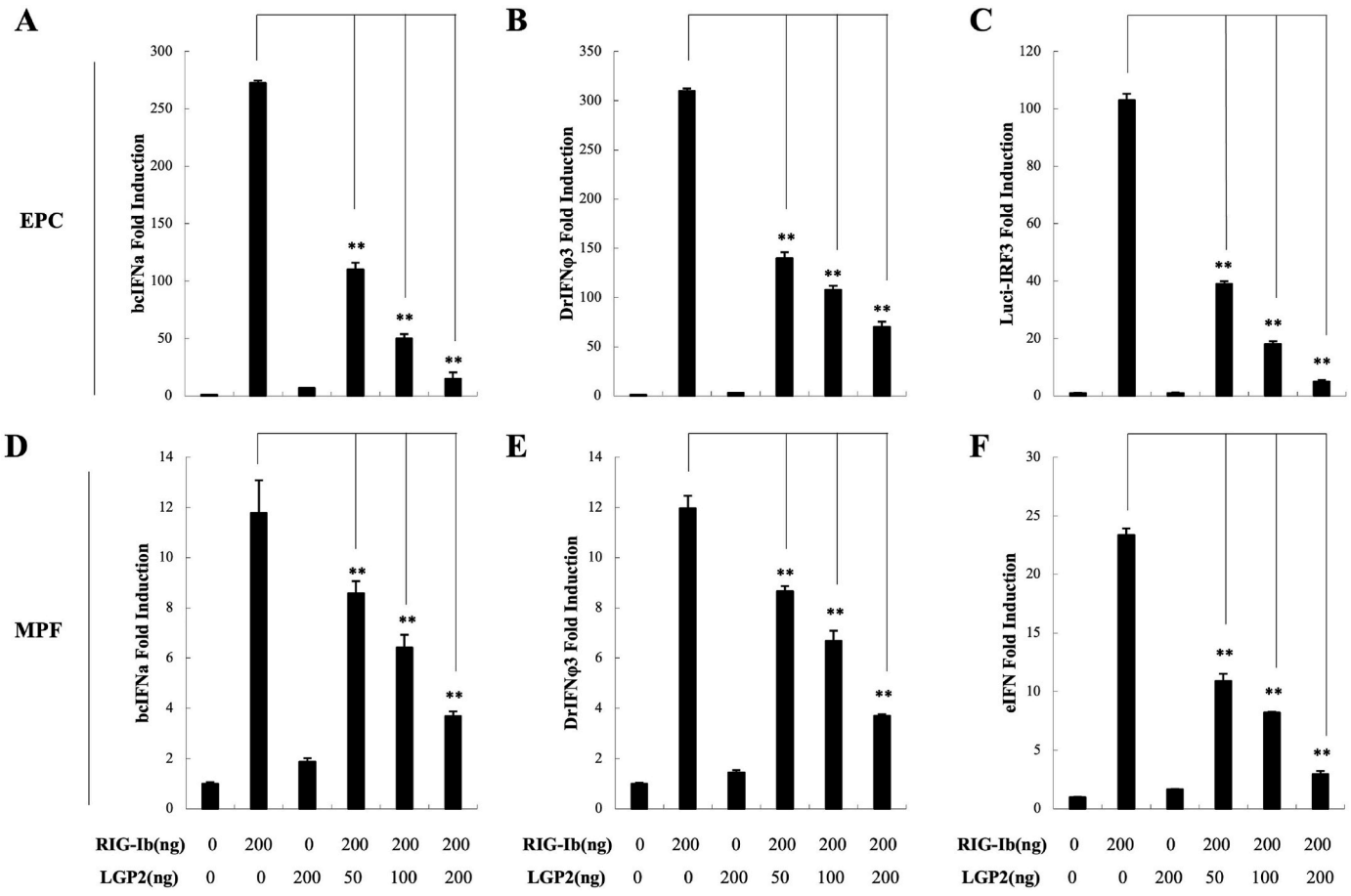


**Fig. 2.** bcLGP2 dampened bcRIG-Ib-mediated IFN transcription. EPC and MPF cells in 24-well plates were co-transfected with pcDNA5, bcRIG-Ib, bcLGP2, pRL-TK, DrIFNφ3, bcIFNa, eIFN or bcIRF3 promoters separately. The cells were harvested at 24h post-transfection and used for dual-luciferase reporter assay. RIG-Ib: pcDNA5-FRT/TO bcRIG-Ib-Flag; LGP2: pcDNA5-FRT/TO HA-bcLGP2. Error bars represent the standard error of the mean (+SEM) of three independent experiments. Data are representative of three independent experiments. *P < 0.05, **P < 0.01.

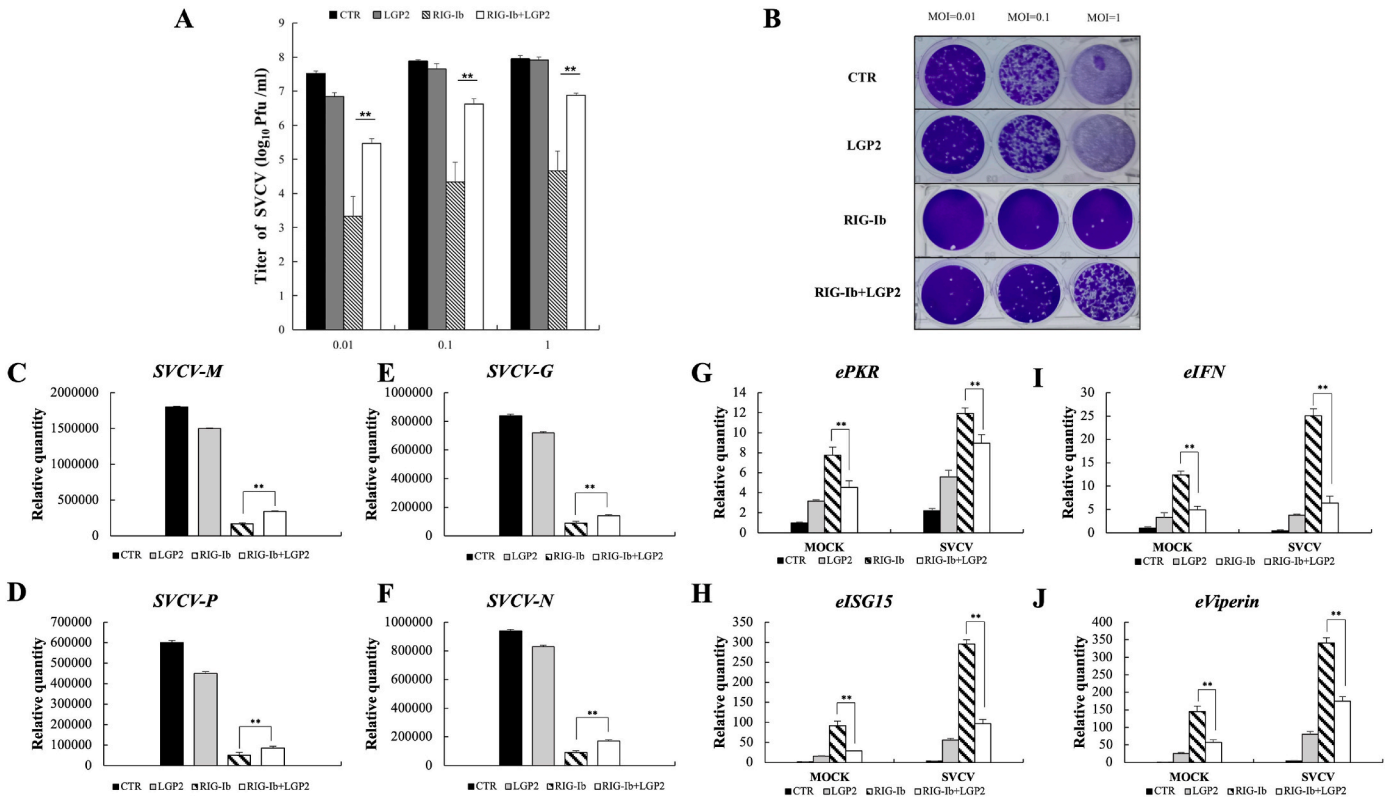


**Fig. 3.** bcLGP2 restricted the antiviral activity of bcRIG-Ib. EPC cells in 24-well plates were co-transfected with bcRIG-Ib and/or bcLGP2, the cells were infected with SVCV at indicated MOIs (0.01/0.1/1) after 24h post-transfection. After 24h post-infection, the supernatant media were collected for plaque assay to examine the SVCV virus titer (A) and the cell monolayers were stained with crystal violet (B). EPC cells in 6-well plates were transfected with pcDNA5, bcRIG-Ib and/or bcLGP2, which were infected with SVCV at MOI = 0.1 for 2 h, then changed the medium including SVCV to 2% FBS culture medium for further 24h culturing. The treated EPC cells were harvested and subjected to RNA extraction and reverse transcription to obtain cDNA and the relative mRNA levels of *SVCV-M* (C), *SVCV-P* (D), *SVCV-G* E, *SVCV-N* (F) *ePKR* (G), *eISG15* (H), *eIFN* (I) and *eViperin* (J) were examined by qRT-PCR assays. CTR: cells were transfected with empty vector pcDNA5-FRT/TO; RIG-Ib: pcDNA5-FRT/TO-bcRIG-Ib-Flag; LGP2: pcDNA5-FRT/TO-HA-bcLGP2; RIG-Ib + LGP2: cells were co-transfected with pcDNA5-FRT/TObcRIG-Ib-Flag and pcDNA5-FRT/TO-HA-bcLGP2. Error bars represent the standard error of the mean (+SEM) of three independent experiments. Data are representative of three independent experiments. *P < 0.05, **P < 0.01.

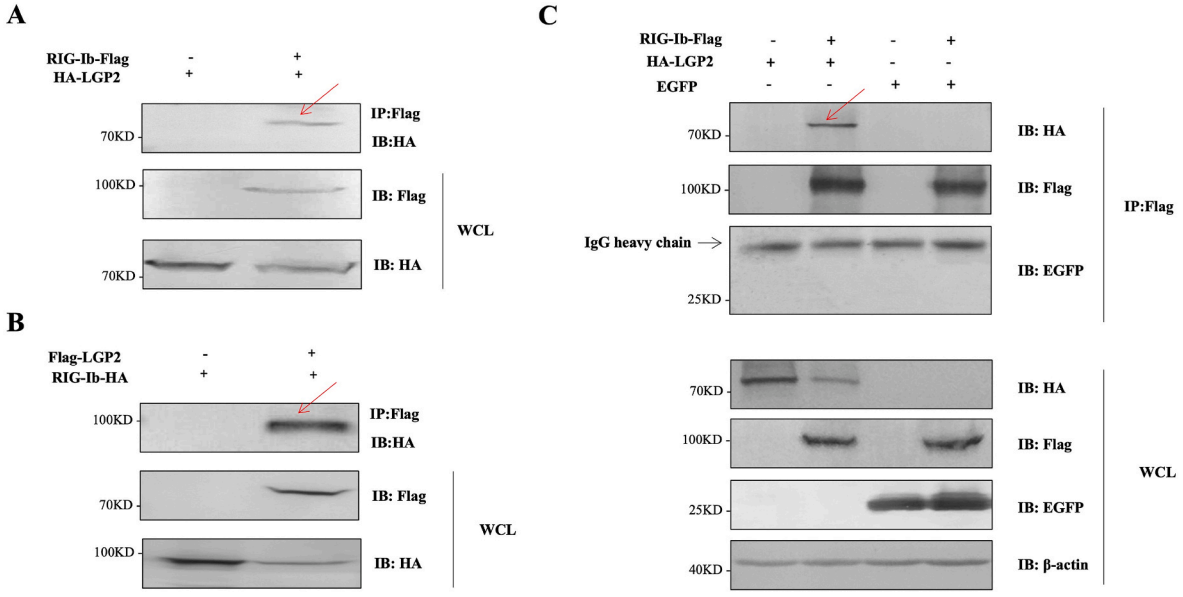


**Fig. 4.** The protein interactions between bcRIG-Ib and bcLGP2. (A–B) Co-immunoprecipitation (co-IP) assays were executed in HEK293T cells with co-transfection of pcDNA5, bcRIG-Ib and/or bcLGP2. (C) Co-immunoprecipitation (co-IP) assays were executed in HEK293T cells with co-transfection of pcDNA5, EGFP, bcRIG-Ib and/or bcLGP2. IP: immunoprecipitation; IB: immunoblotting; WCL: whole cell lysates; RIG-Ib-Flag: pcDNA5-FRT/TO-bcRIG-Ib-Flag; HA-LGP2: pcDNA5-FRT/TO-HA-bcLGP2; Flag-LGP2: pcDNA5-FRT/TO-Flag-bcLGP2; RIG-Ib-HA: pcDNA5-FRT/TO-bcRIG-Ib-HA; EGFP: pEGFP-N1.

plasmids simultaneously and then subjected to co-IP assays. The co-IP assay results display the specific band (Fig. 4A red arrow indicated) representing HA-bcLGP2 (~72 kDa) was detected in the precipitated proteins by bcRIG-Ib-Flag, while the specific band (Fig. 4B red arrow indicated) representing bcRIG-Ib-HA(~100 kDa) was also detected in the precipitated proteins by Flag-bcLGP2. To offset the false positive results may occur, we further conducted a co-IP assay with an unrelated protein, EGFP, as a control group. As shown in Fig. 4C, there is no specific band been detected in the precipitated proteins in EGFP group, but a specific band (the red arrow indicated) representing bcLGP2 (~72 kDa) was detected. The above data collectively confirmed the interaction between bcLGP2 and bcRIG-Ib.

### 3.5. DExD/H-box helicase domain of bcLGP2 possesses the dominant inhibition on bcRIG-Ib

Our previous studies have identified two functional domains in bcLGP2: N-terminus DExD/H-box Helicase (3-473aa) and CTD domain (553-665aa) [29]. To identify the functional regions of bcLGP2 negatively regulating bcRIG-Ib, we constructed four different mutants of bcLGP2 plasmids: bcLGP2-Helicase (bcLGP2 mutational plasmid only contains DExD/H-box Helicase domain), bcLGP2-CTD (bcLGP2 mutational plasmid only contains CTD domain), bcLGP2-ΔHelicase (bcLGP2 mutational plasmid with DExD/H-box Helicase domain deletion), and bcLGP2-ΔCTD (bcLGP2 mutational plasmid with CTD domain deletion) (Fig. 5A). These recombinant truncated bcLGP2 plasmids were transfected into HEK293T cells separately and then subjected to SDS-PAGE electrophoresis. The immunoblotting (IB) assay results showed that all these plasmids were successfully expressed in HEK293T (Fig. 5B).

To explore the functional roles of bcLGP2 mutants in bcRIG-Ib-mediated IFN promoter transcription activity, we co-transfected bcRIG-Ib with bcLGP2, bcLGP2-Helicase, bcLGP2-CTD, bcLGP2-ΔHelicase, or bcLGP2-ΔCTD separately, and then performed the dual-luciferase reporter assays to measure the activation level of different fish IFN promoters, including bcIFNa-pro (Fig. 5C), eIFN-pro (Fig. 5D), DrIFNφ1-pro (Fig. 5E), and DrIFNφ3-pro (Fig. 5F). The results indicated that bcLGP2-Helicase and bcLGP2-ΔCTD significantly inhibit the bcRIG-Ib-mediated IFN promoter transcriptions to a similar extent as the full-length bcLGP2, while bcLGP2-CTD and bcLGP2-ΔHelicase do not demonstrate such inhibition. Thus, we concluded that the DExD/H-box Helicase domain of bcLGP2 possessed the dominant inhibition on bcRIG-Ib.

### 3.6. Protein interaction and down-regulated antiviral ability between bcLGP2 and bcRIG-Ib-CARD

In mammals, the CARDs domain of mammalian RIG-I were known to trigger downstream antiviral signaling cascades, mimicking full-length activated RIG-I [4,10]. Structural and functional analysis of bcRIG-Ib in our lab demonstrated that the CARDs domain of bcRIG-Ib was crucial for bcRIG-Ib-mediated antiviral signaling [37]. Thus, we next explored whether bcLGP2 functions on CARDs to inhibit the function of bcRIG-Ib. The co-IP results showed that bcLGP2 interacts with bcRIG-Ib-CARD (Fig. 6A the red arrow indicated). Furthermore, in antiviral experiments, we found that the viral titers in the cells co-expressing bcRIG-Ib-CARD and bcLGP2 were much higher than those in the cells

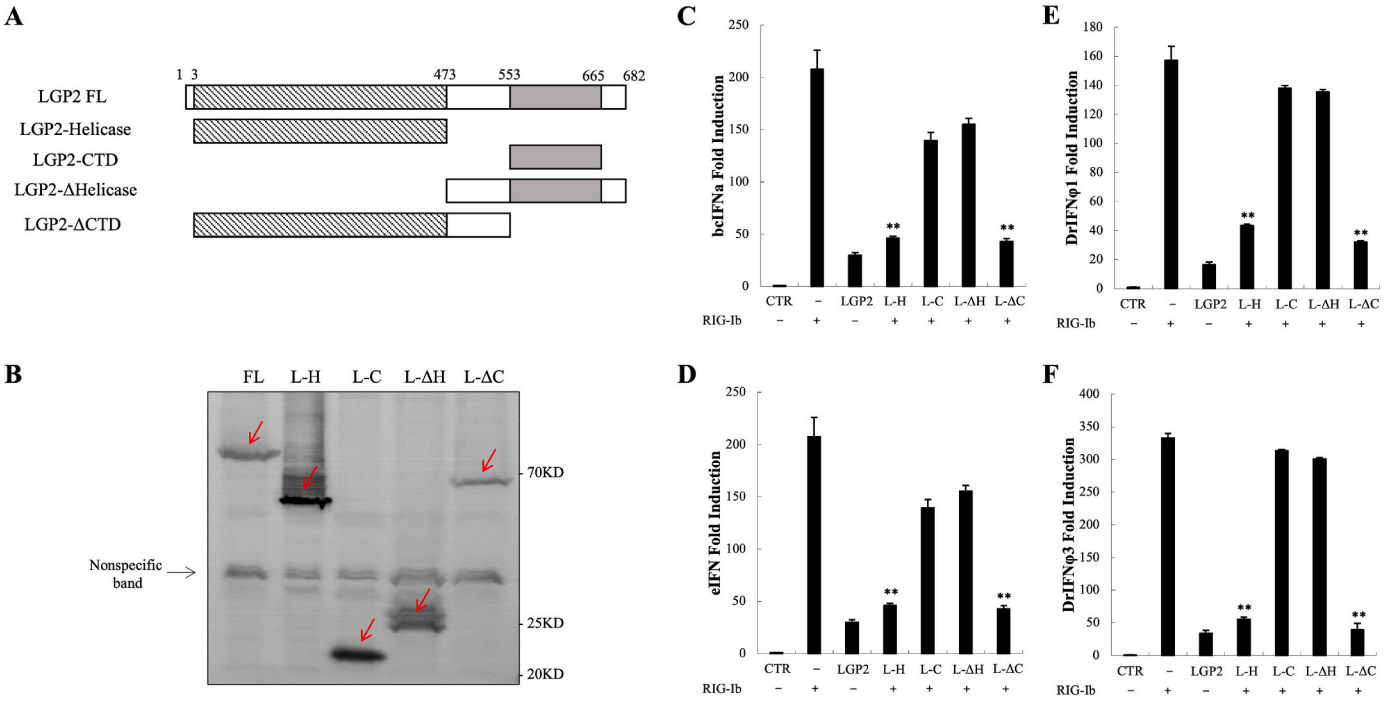


**Fig. 5.** DExD/H-box Helicase domain of bcLGP2 possesses the dominant inhibition on bcRIG-Ib. Schematic diagram of the predicted domain within bcLGP2 and truncational mutants of bcLGP2. LGP2 FL: full-length bcLGP2; LGP2-Helicase: bcLGP2 recombinant plasmid only possesses DExD/H-box-box Helicase domain (3-473aa); LGP2-CTD: bcLGP2 recombinant plasmid only possesses C-terminus domain (553-665aa); LGP2-ΔHelicase: bcLGP2 recombinant plasmid with DExD/H-box-box Helicase domain deletion (474-682aa); LGP2-ΔCTD: bcLGP2 recombinant plasmid with C-terminus domain deletion (3-552aa). (A) HEK293T cells in 6-well plates were transfected with LGP2 FL, LGP2-Helicase, LGP2-CTD, LGP2-ΔHelicase and LGP2-ΔCTD plasmids respectively and collected for immunoblotting (IB) assays. (C–F) EPC cells in 24-well plates were co-transfected with pcDNA5, bcRIG-Ib, bcLGP2, LGP2-Helicase, LGP2-CTD, LGP2-ΔHelicase and LGP2-ΔCTD plasmids, together with pRL-TK and bcIFNa/epcIFN/DrIFNφ3/DrIFNφ1 promoters. The cells were harvested after 24 hpt and subjected to dual-luciferase reporter assay. CTR: cells were transfected with empty vector pcDNA5-FRT/TO; RIG-Ib: pcDNA5-FRT/TO-bcRIG-Ib-Flag; LGP2: pcDNA5-FRT/TO-HA-bcLGP2; L–H: the recombinant expression vector pcDNA5/FRT/TO-HA-bcLGP2-Helicase; L–C: pcDNA5/FRT/TO-HA-bcLGP2-CTD; L-ΔH: pcDNA5/FRT/TO-HA-bcLGP2-ΔHelicase; L-ΔC: pcDNA5/FRT/TO-HA-bcLGP2-ΔCTD. Error bars represent the standard error of the mean (+SEM) of three independent experiments. Data are representative of three independent experiments. *P < 0.05, **P < 0.01.

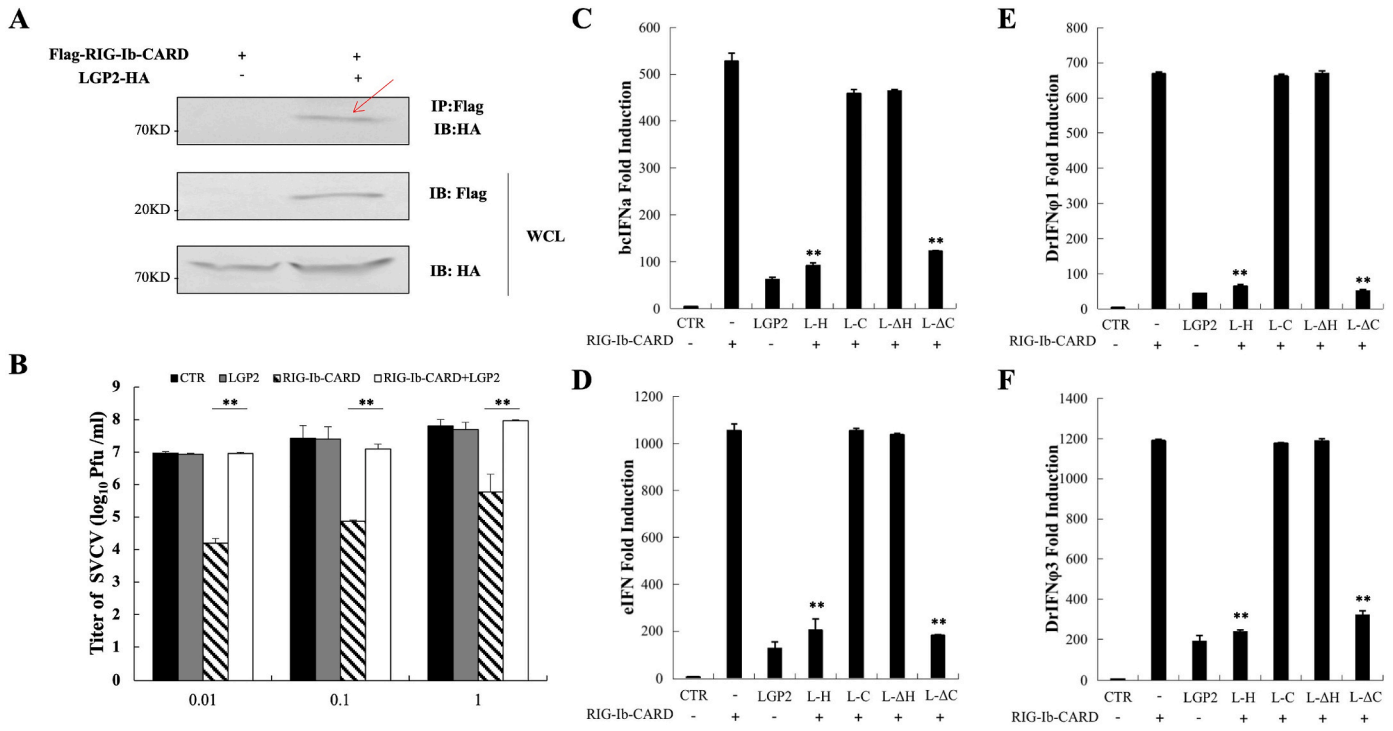


**Fig. 6.** The protein interaction and down-regulation of antiviral ability between bcLGP2 and bcRIG-Ib-CARD. (A) Co-immunoprecipitation (co-IP) assays were executed in HEK293T cells with co-transfection of bcRIG-Ib-CARD and/or bcLGP2. IP: immunoprecipitation; IB: immunoblotting; WCL: whole cell lysates; Flag-RIG-Ib-CARD: pcDNA5-FRT/TO-Flag-bcRIG-Ib-CARD; LGP2-HA: pcDNA5-FRT/TO-bcLGP2-HA; (B) EPC cells in 24-well plates were transfected with bcRIG-Ib-CARD and/or bcLGP2. The cells were infected with SVCV at indicated MOIs after 24h post-transfection for 2 h, then changed the medium including SVCV to 2%FBS culture medium for further culturing 24h; Then collected the supernatant for plaque assay to examine the SVCV virus titer at 48h post transfection. (C–F) EPC cells in 24-well plates were co-transfected with bcRIG-Ib-CARD, bcLGP2, LGP2-Helicase, LGP2-CTD, LGP2-ΔHelicase and LGP2-ΔCTD plasmids, together with pRL-TK and bcIFNa/epcIFN/DrIFNφ3/DrIFNφ1 promoters. The cells were harvested after 24h post-transfection and subjected to dual-luciferase reporter assay. CTR: cells were transfected with empty vector pcDNA5-FRT/TO; RIG-Ib-CARD: pcDNA5-FRT/TO-Flag-bcRIG-Ib-CARD; LGP2: pcDNA5-FRT/TO-HA-bcLGP2; L–H: the recombinant expression vector pcDNA5/FRT/TO-HA-bcLGP2-Helicase; L–C: pcDNA5/FRT/TO-HA-bcLGP2-CTD; L-ΔH: pcDNA5/FRT/TO-HA-bcLGP2-ΔHelicase; L-ΔC: pcDNA5/FRT/TO-HA-bcLGP2-ΔCTD. Error bars represent the standard error of the mean (+SEM) of three independent experiments. Data are representative of three independent experiments. *P < 0.05, **P < 0.01.

expressing bcRIG-Ib-CARD alone (Fig. 6 B). These data corporately suggested that bcLGP2 not only interacts with bcRIG-Ib-CARD but also straightforwardly inhibits the bcRIG-Ib-CARD-mediated antiviral ability against SVCV.

Based on the association between bcRIG-Ib-CARD and bcLGP2, we further investigated whether different regions of bcLGP2 execute disparate functions on bcRIG-Ib-CARD. We co-transfected bcRIG-Ib-CARD with different bcLGP2 mutant plasmids into EPC cells and then performed dual-luciferase reporter assays. The results showed that the activation levels of bcIFNa-pro (Fig. 6C), eIFN-pro (Fig. 6D), DrIFNφ1-pro (Fig. 6E), and DrIFNφ3-pro (Fig. 6F) which induced by bcRIG-Ib-CARD were significantly reduced by bcLGP2-Helicase and bcLGP2-ΔCTD. Thus, these results suggest that the DExD/H-box Helicase domain of bcLGP2 plays a dominantly inhibitory role in the bcRIG-Ib-CARD-mediated IFN signaling pathway.

### *3.7. bcLGP2 mediated proteasomal degradation of bcRIG-Ib by enhancing its K48-linked ubiquitination*

According to the results of Fig. 4, we noticed that overexpression of bcLGP2 led to a decrease in protein level of bcRIG-Ib, while overexpression of bcRIG-Ib also inhibited the protein level of bcLGP2. Thus, we further investigated the underlying mechanism. Since the ubiquitin-proteasome pathway is one of the major mechanisms responsible for protein degradation, we first explored whether bcLGP2 will affect the ubiquitination level of bcRIG-Ib [38,39]. As shown in Fig. 7A, compared to the group that bcRIG-Ib was transfected alone, the wild-type and K48-linked ubiquitination of bcRIG-Ib in the group co-expressing bcRIG-Ib and bcLGP2 was significantly enhanced. However, the K63-linked ubiquitination levels of bcRIG-Ib did not differ obviously. These results implied that bcLGP2 may promote bcRIG-Ib degradation through the ubiquitin-proteasome pathway. To further confirm it, we treated the cells co-expressing bcLGP2 and bcRIG-Ib using the proteasomal inhibitor MG132 or lysosomal inhibitor chloroquine diphosphate (CQ). The IB assay and relative grey value analysis results revealed that the decreased protein levels both of bcRIG-Ib (Fig. 7B) and bcLGP2 (Fig. 7C) were restored after MG132 treatment, rather than CQ treatment. Overall, the findings suggest that bcLGP2 enhances the K48-linked ubiquitination of bcRIG-Ib, which in turn promotes the proteasomal degradation of bcRIG-Ib.

## 4. Discussion

RLRs are known to localize in the cytosol and to be tightly regulated by host regulatory mechanisms, including RLR-interacting proteins, post-translational modifications, and non-coding RNAs [40]. The key sensor of RLRs, RIG-I, mediates downstream signal cascade transmission and increases transcriptional induction of type I interferons and ISGs that collectively initiate antiviral response [15]. RIG-I characteristically monitors dsRNAs with 5′-triphosphate (5′PPP) ends by DExD/H-box Helicase domain and CTD, then transmits signals downstream through two CARDs [5]. RIG-I monomers stay inactive stage in resting cells, CARDs are inhibited by the CTD. When encountering viral infection, RIG-I shifts conformation, promoting self-association and releasing CARDs from CTD to interact with MAVS. MAVS is encompassed in the CARD family, mediating CARD-dependent interactions with RIG-I and

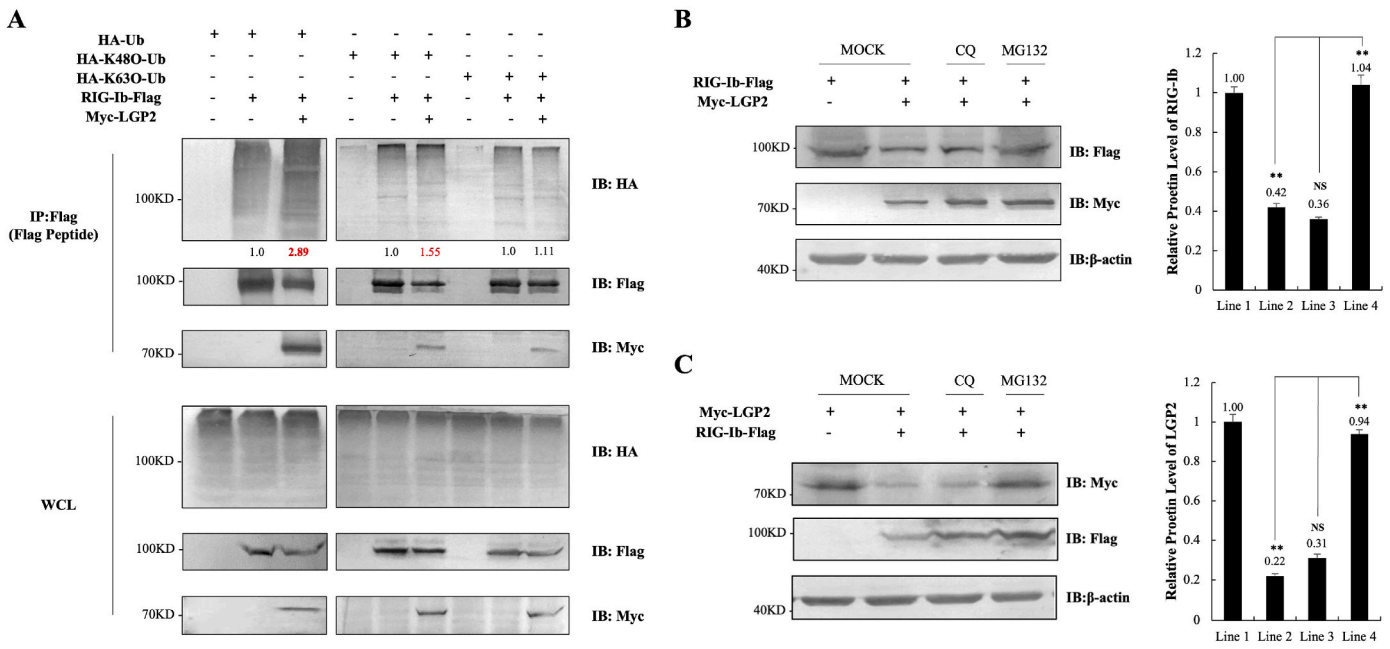


**Fig. 7.** bcLGP2 mediated proteasomal degradation of bcRIG-Ib through enhancing its K48-linked ubiquitination. (A) HEK293T cells were co-transfected with HA-Ub, HA- K48O-Ub, HA-K63O-Ub, bcRIG-Ib and/or bcLGP2 separately and harvested for co-immunoprecipitation (co-IP) assays at 48h post-transfection. (B–C) HEK293T cells were transfected with bcRIG-Ib and/or bcLGP2, then treated with MG132 (10 μM) or CQ (50 μM) individually at 36h post-transfection for 12h treatments then harvested for immunoblotting (IB) assays. The detected relative protein levels were analyzed by ImageJ with presented histograms. IP: immunoprecipitation; IB: immunoblotting; WCL: whole cell lysates; HA-Ub: pcDNA5/FRT/TO-HA-Ub; HA-K48O-Ub: pcDNA5/FRT/TO-HA-K48O-Ub; HA-K63O-Ub: pcDNA5/FRT/TO-HA-K63O-Ub; RIG-Ib-Flag: pcDNA5-FRT/TO-bcRIG-Ib-Flag; Myc-LGP2: pcDNA5-FRT/TO-Myc-bcLGP2; Error bars represent the standard error of the mean (+SEM) of three independent experiments. Data are representative of three independent experiments. *P < 0.05, **P < 0.01.

MDA5. As a vital adaptor protein, MAVS activates the downstream signals to induce IFNs and antiviral molecules to fight against viral invasion [41–45]. However, recent studies have reported that both viral and self-derived RNAs could trigger host cellular RLRs, leading to a two-sided phenomenon that although effective antiviral responses could be established, it may also lead to uncontrolled immunopathology. Misregulation of RIG-I could deleteriously influence the antiviral host response [41]. To maintain a well-organized homeostasis stage, it is pivotal to keep the mechanisms of RLRs undergoing restrictive regulations.

Although LGP2 lacks the N-terminal tandem CARDs, it still regulates the signaling transduction of RIG-I and MDA5. For example, LGP2 has been reported to play both positive and negative regulatory roles on RIG-I and MDA5. LGP2 negatively regulates RIG-I-induced antiviral signaling, the CTD in LGP2 is necessary to bind with CARDs and DExD/H-box Helicase in RIG-I [41]. LGP2 sometimes acts as a feedback inhibitory element of RIG-I, prevents RIG-I from MAVS association, and lessens the ubiquitination of RIG-I [46,47]. While LGP2 assists MDA5 antiviral response: LGP2-knockout mice were more susceptible to the infection of EMCV (a kind of RNA virus mainly recognized by MDA5) [21,22]. Besides, the cells derived from LGP2-deficient mice failed to initiate effective antiviral responses after EMCV infection. It is believed that LGP2 cooperates with MDA5 filaments and enhances the association between MDA5 and RNAs, promoting MDA5-RNA filament formation, and ultimately amplifies the antiviral function of MDA5 [17,20,48].

The fish RLRs share protein domains with mammalian RLRs, including DExD/H-box Helicase and CTD. However, LGP2 lacks tandem CARDs. All three members can be stimulated *in vivo* and *in vitro* by viral infections or poly(I:C), leading to the induction of type I IFNs and antiviral molecules [49]. Fish LGP2 consistently plays a dually modulatory role within RIG-I and MDA5. In grass carp, LGP2 negatively regulates RIG-I and MDA5 at resting state and early stage of GCRV infection in CIK cells; LGP2 restrains K63 and K48 linked ubiquitination of RIG-I and MDA5 in various degrees [24]. LGP2 loss-of-function ($lgp2^{lof/lof}$) zebrafish is more susceptible to SVCV infection, displaying a decreased antiviral response and a following increased one; zebrafish LGP2 positively regulates MDA5 in SVCV infected early stage, and then LGP2 presents as an inhibitor of TBK1 and IKKε at late stage of SVCV infection. Furthermore, the cellular IFN production and over-expression transfection dose of LGP2 is crucial for its accurate function in EPC cells: a relatively low dose of zebrafish LGP2 initiates strong IFN transcriptions and induction of PKR and IRF3 proteins, but diminishes in a high dose of zebrafish LGP2 [25]. Our previous study demonstrated that black carp LGP2 functions as a positive regulator of MDA5. Black carp MDA5 induced obviously increasing IFN expression and owned much improved antiviral ability with the presence of LGP2 [50].

In this paper, we further explored the role of black carp LGP2 in regulating bcRIG-Ib. Knockdown of bcLGP2 attenuated the antiviral capability of host cells (Fig. 1), which is in accord with our previous study on bcLGP2: bcLGP2 enhanced the host celluar antiviral ability [29]. Co-transfection of bcRIG-Ib and bcLGP2 caused severely impaired transcription of type I IFNs and interferon-stimulated genes (ISGs), resulting in the loss of restraints on SVCV replication (Fig. 2). Besides, bcLGP2 potently inhibited bcRIG-Ib/bcRIG-Ib-CARD mediated antiviral ability, leading to an increased viral load (Fig. 3). The interaction between bcLGP2 and bcRIG-Ib/bcRIG-Ib-CARD was detected (Fig. 4) *in vitro*. DExD/H-box Helicase domain in bcLGP2 possessed a similar inhibitory effect on bcRIG-Ib/bcRIG-Ib-CARD to that of full-length bcLGP2, while the CTD of bcLGP2 presented little impact on bcRIG-Ib/bcRIG-Ib-CARD (Figs. 5 and 6). The co-IP assays showed that the K63-linked ubiquitination levels were similar in both the bcRIG-Ib singly expressed group and bcLGP2/bcRIG-Ib co-expressed group. However, the wild-type and K48-linked ubiquitination level of bcLGP2/bcRIG-Ib co-expressed group was relevantly increased by 2.89-folds and 1.55-folds separately (Fig. 7A). These data suggested that the impaired bcRIG-Ib protein level was conducted by K48-linked ubiquitination, promoting proteasomal degradation of bcRIG-Ib [38,51].

Although bcLGP2 is not an E3 ubiquitin ligase, it still conducts heightened ubiquitin levels on bcRIG-Ib in our results. We believe that bcLGP2 needs to rely on other E3 ubiquitin ligases to modify bcRIG-I, thereby enhancing the ubiquitination of bcRIG-Ib. For instance, in mammals, RIG-I was modified by the E3 ubiquitin ligase RNF122, resulting in an increase in ubiquitination of its K48-linked ubiquitination and its proteasomal degradation [38]. Therefore, in this study, which E3 ubiquitin ligase is utilized by bcLGP2 to mediate the degradation of bcRIG-I remains to be explored further. Interestingly, we observed that bcRIG-Ib can also inhibit the protein level of bcLGP2 through the proteasome pathway. Therefore, we speculated that bcRIG-Ib might act as a negative feedback element of bcLGP2, reversely inhibiting the protein level of bcLGP2, aiming to maintain bcRIG-Ib itself a sufficient cytosolic concentration.

In this research, we proposed that bcLGP2 alone enhanced host cellular antiviral capacity, but when it co-expressed with bcRIG-Ib, it suppressed bcRIG-Ib-mediated IFN signaling. We think that bcLGP2 may play a role in balancing the innate homeostasis immune response. During viral infection, the relative expression levels of RIG-I and MDA5, and their functional status, the binding affinities with LGP2 may differ to a large extent, resulting in differences in signal transductions and antiviral responses. The presence of LGP2 may play a curial regulatory role between RLRs, thereby triggering appropriate innate immune responses. For example, in this study, we demonstrated that bcLGP2 inhibited bcRIG-Ib mediated IFN signaling by regulating the post-translational modifications of bcRIG-Ib, such as ubiquitination, which is a manifestation of bcLGP2's function in avoiding excessive immune activation. On the other hand, in our previous study on black carp MDA5 and LGP2, we found that bcLGP2 itself has antiviral ability, and it can also significantly enhance the bcMDA5-mediated antiviral activity. This is a manifestation of bcLGP2 promoting the host's innate immune response function. These results collectively indicate that bcLGP2 plays a dual role in the antiviral innate immune response. Another study in zebrafish also showed that LGP2 is crucial for zebrafish to resist SVCV infection and it plays a dual regulatory role in host innate immunity: DrLGP2 functions as a positive regulator dependent on MDA5 and a negative one by impairing TBK1 and IKKε mRNA levels. Therefore, DrLGP2 is a key homeostatic regulator of IFN response during virus infection [25]. In conclusion, bcLGP2, as a regulatory protein that can interact with both bcRIG-I and bcMDA5, plays a critical role in balancing innate homeostasis of immune and inflammatory response in black carp. However, the specific mechanism of bcLGP2 during different viral infections and molecules needs further research to reveal the implications within the innate immune system of vertebrates.

## CRediT authorship contribution statement

**Yixuan He:** Investigation, Writing – original draft. **Ji Liu:** Methodology, Visualization. **Yujia Miao:** Visualization. **Meiling Liu:** Software. **Hui Wu:** Investigation, Methodology. **Jun Xiao:** Conceptualization, writing-reviewing. **Hao Feng:** Supervision, Project administration, editing.

## Data availability

Data will be made available on request.

## Acknowledgements

This work was supported by the National Natural Science Foundation of China (U21A20268, 31920103016, 32002415, 32002383), Hunan Provincial Science and Technology Department (2022JJ40271, 2023JJ40435), the Modern Agricultural Industry Program of Hunan Province, the Research and Development Platform of Fish Disease and Vaccine for Postgraduates in Hunan Province.

## References

[1] D.C. Beachboard, S.M. Horner, Innate immune evasion strategies of DNA and RNA viruses, Curr. Opin. Microbiol. 32 (2016) 113–119.
[2] S. Akira, S. Uematsu, O. Takeuchi, Pathogen recognition and innate immunity, Cell 124 (4) (2006) 783–801.
[3] O. Takeuchi, S. Akira, Pattern recognition receptors and inflammation, Cell 140 (6) (2010) 805–820.
[4] M. Yoneyama, M. Kikuchi, T. Natsukawa, N. Shinobu, T. Imaizumi, M. Miyagishi, K. Taira, S. Akira, T. Fujita, The RNA helicase RIG-I has an essential function in double-stranded RNA-induced innate antiviral responses, Nat. Immunol. 5 (7) (2004) 730–737.
[5] V. Hornung, J. Ellegast, S. Kim, K. Brzozka, A. Jung, H. Kato, H. Poeck, S. Akira, K. K. Conzelmann, M. Schlee, S. Endres, G. Hartmann, 5'-Triphosphate RNA is the ligand for RIG-I, Science 314 (5801) (2006) 994–997.
[6] A. Kohlway, D.H. Luo, D.C. Rawling, S.C. Ding, A.M. Pyle, Defining the functional determinants for RNA surveillance by RIG-I, EMBO Rep. 14 (9) (2013) 772–779.
[7] T. Saito, D.M. Owen, F. Jiang, J. Marcotrigiano, M. Gale Jr., Innate immunity induced by composition-dependent RIG-I recognition of hepatitis C virus RNA, Nature 454 (7203) (2008) 523–527.
[8] E. Kowalinski, T. Lunardi, A.A. McCarthy, J. Louber, J. Brunel, B. Grigorov, D. Gerlier, S. Cusack, Structural basis for the activation of innate immune pattern-recognition receptor RIG-I by viral RNA, Cell 147 (2) (2011) 423–435.
[9] D. Luo, S.C. Ding, A. Vela, A. Kohlway, B.D. Lindenbach, A.M. Pyle, Structural insights into RNA recognition by RIG-I, Cell 147 (2) (2011) 409–422.
[10] D. Thoresen, W. Wang, D. Galls, R. Guo, L. Xu, A.M. Pyle, The molecular mechanism of RIG-I activation and signaling, Immunol. Rev. 304 (1) (2021) 154–168.
[11] Q. Sun, L. Sun, H.H. Liu, X. Chen, R.B. Seth, J. Forman, Z.J. Chen, The specific and essential role of MAVS in antiviral innate immune responses, Immunity 24 (5) (2006) 633–642.
[12] S.K. Saha, E.M. Pietras, J.Q. He, J.R. Kang, S.Y. Liu, G. Oganesyan, A. Shahangian, B. Zarnegar, T.L. Shiba, Y. Wang, G. Cheng, Regulation of antiviral responses by a direct and specific interaction between TRAF3 and Cardif, EMBO J. 25 (14) (2006) 3257–3263.
[13] R.B. Seth, L. Sun, C.K. Ea, Z.J. Chen, Identification and characterization of MAVS, a mitochondrial antiviral signaling protein that activates NF-kappaB and IRF 3, Cell 122 (5) (2005) 669–682.
[14] J. Hiscott, R. Lin, P. Nakhaei, S. Paz, MasterCARD: a priceless link to innate immunity, Trends Mol. Med. 12 (2) (2006) 53–56.
[15] J. Rehwinkel, M.U. Gack, RIG-I-like receptors: their regulation and roles in RNA sensing, Nat. Rev. Immunol. 20 (9) (2020) 537–551.
[16] K.R. Rodriguez, A.M. Bruns, C.M. Horvath, MDA5 and LGP2: accomplices and antagonists of antiviral signal transduction, J. Virol. 88 (15) (2014) 8194–8200.
[17] I. Duic, H. Tadakuma, Y. Harada, R. Yamaue, K. Deguchi, Y. Suzuki, S. H. Yoshimura, H. Kato, K. Takeyasu, T. Fujita, Viral RNA recognition by LGP2 and MDA5, and activation of signaling through step-by-step conformational changes, Nucleic Acids Res. 48 (20) (2020) 11664–11674.
[18] M. Yoneyama, M. Kikuchi, K. Matsumoto, T. Imaizumi, M. Miyagishi, K. Taira, E. Foy, Y.M. Loo, M. Gale Jr., S. Akira, S. Yonehara, A. Kato, T. Fujita, Shared and unique functions of the DExD/H-box helicases RIG-I, MDA5, and LGP2 in antiviral innate immunity, J. Immunol. 175 (5) (2005) 2851–2858.
[19] R.Y. Sanchez David, C. Combredet, V. Najburg, G.A. Millot, G. Beauclair, B. Schwikowski, T. Leger, J.M. Camadro, Y. Jacob, J. Bellalou, N. Jouvenet, F. Tangy, A.V. Komarova, LGP2 binds to PACT to regulate RIG-I- and MDA5-mediated antiviral responses, Sci. Signal. 12 (601) (2019).
[20] K. Esser-Nobis, L.D. Hatfield, M. Gale Jr., Spatiotemporal dynamics of innate immune signaling via RIG-I-like receptors, Proc. Natl. Acad. Sci. U. S. A. 117 (27) (2020) 15778–15788.
[21] T. Satoh, H. Kato, Y. Kumagai, M. Yoneyama, S. Sato, K. Matsushita, T. Tsujimura, T. Fujita, S. Akira, O. Takeuchi, LGP2 is a positive regulator of RIG-I- and MDA5-mediated antiviral responses, Proc. Natl. Acad. Sci. U. S. A. 107 (4) (2010) 1512–1517.
[22] T. Venkataraman, M. Valdes, R. Elsby, S. Kakuta, G. Caceres, S. Saijo, Y. Iwakura, G.N. Barber, Loss of DExD/H box RNA helicase LGP2 manifests disparate antiviral responses, J. Immunol. 178 (10) (2007) 6444–6455.
[23] D. Chopy, J. Pothlichet, M. Lafage, F. Megret, L. Fiette, M. Si-Tahar, M. Lafon, Ambivalent role of the innate immune response in rabies virus pathogenesis, J. Virol. 85 (13) (2011) 6657–6668.
[24] Y. Rao, Q. Wan, C. Yang, J. Su, Grass carp laboratory of genetics and physiology 2 serves as a negative regulator in retinoic acid-inducible gene I- and melanoma differentiation-associated gene 5-mediated antiviral signaling in resting state and early stage of grass carp reovirus infection, Front. Immunol. 8 (2017) 352.
[25] X.Y. Gong, Q.M. Zhang, X. Zhao, Y.L. Li, Z.L. Qu, Z. Li, C. Dan, J.F. Gui, Y.B. Zhang, LGP2 is essential for zebrafish survival through dual regulation of IFN antiviral response, iScience 25 (8) (2022), 104821.
[26] T. Takahashi, Y. Nakano, K. Onomoto, M. Yoneyama, K. Ui-Tei, LGP2 virus sensor enhances apoptosis by upregulating apoptosis regulatory genes through TRBP-bound miRNAs during viral infection, Nucleic Acids Res. 48 (3) (2020) 1494–1507.
[27] W. Zheng, D.R.E. Ranoa, X. Huang, Y. Hou, K. Yang, E.C. Poli, M.A. Beckett, Y. X. Fu, R.R. Weichselbaum, RIG-I-Like receptor LGP2 is required for tumor control by radiotherapy, Cancer Res. 80 (24) (2020) 5633–5641.
[28] P.F. Zou, M.X. Chang, Y. Li, S. Huan Zhang, J.P. Fu, S.N. Chen, P. Nie, Higher antiviral response of RIG-I through enhancing RIG-I/MAVS-mediated signaling by its long insertion variant in zebrafish, Fish Shellfish Immunol. 43 (1) (2015) 13–24.

[29] J. Xiao, J. Yan, H. Chen, J. Li, Y. Tian, H. Feng, LGP2 of black carp plays an important role in the innate immune response against SVCV and GCRV, Fish Shellfish Immunol. 57 (2016) 127–135.
[30] T. Xue, Y.Z. Wang, Q.H. Pan, Q. Wang, J.F. Yuan, T.S. Chen, Establishment of a cell line from the kidney of black carp and its susceptibility to spring viremia of carp virus, J. Fish. Dis. 41 (2) (2018) 365–374.
[31] Q. Wang, Y. Ai, C. Wang, Y. Liu, H. Zhong, W. Yan, Y. He, Z. Deng, J. Zou, H. Feng, PKACα negatively regulates TAK1/IRF7 signaling in black carp Mylopharyngodon piceus, Dev. Comp. Immunol. 127 (2022), 104306.
[32] W. Zhou, J. Zhou, Y. Lv, Y. Qu, M. Chi, J. Li, H. Feng, Identification and characterization of MAVS from black carp Mylopharyngodon piceus, Fish Shellfish Immunol. 43 (2) (2015) 460–468.
[33] Z. Huang, S. Chen, J. Liu, J. Xiao, J. Yan, H. Feng, IFNa of black carp is an antiviral cytokine modified with N-linked glycosylation, Fish Shellfish Immunol. 46 (2) (2015) 477–485.
[34] X. Dong, H. Feng, Q. Sun, H. Li, T.T. Wu, R. Sun, S.A. Tibbetts, Z.J. Chen, P. Feng, Murine gamma-herpesvirus 68 hijacks MAVS and IKKbeta to initiate lytic replication, PLoS Pathog. 6 (7) (2010), e1001001.
[35] K.J. Livak, T.D. Schmittgen, Analysis of relative gene expression data using real-time quantitative PCR and the 2(-Delta Delta C(T)) Method, Methods 25 (4) (2001) 402–408.
[36] J. Li, Y. Tian, J. Liu, C. Wang, C. Feng, H. Wu, H. Feng, Lysine 39 of IKKepsilon of black carp is crucial for its regulation on IRF7-mediated antiviral signaling, Fish Shellfish Immunol. 77 (2018) 410–418.
[37] J. Liu, Y. He, Y. Miao, C. Dai, J. Yan, M. Liu, J. Zou, H. Feng, The phenylalanine-28 is crucial for black carp RIG-I mediated antiviral signaling, Dev. Comp. Immunol. 148 (2023), 104917.
[38] W. Wang, M. Jiang, S. Liu, S. Zhang, W. Liu, Y. Ma, L. Zhang, J. Zhang, X. Cao, RNF122 suppresses antiviral type I interferon production by targeting RIG-I CARDs to mediate RIG-I degradation, Proc. Natl. Acad. Sci. U. S. A. 113 (34) (2016) 9581–9586.
[39] K. Kato, S. Ahmad, Z. Zhu, J.M. Young, X. Mu, S. Park, H.S. Malik, S. Hur, Structural analysis of RIG-I-like receptors reveals ancient rules of engagement between diverse RNA helicases and TRIM ubiquitin ligases, Mol. Cell 81 (3) (2021) 599–613 e8.
[40] D. Goubau, S. Deddouche, C. Reis e Sousa, Cytosolic sensing of viruses, Immunity 38 (5) (2013) 855–869.
[41] T. Saito, R. Hirai, Y.M. Loo, D. Owen, C.L. Johnson, S.C. Sinha, S. Akira, T. Fujita, M. Gale Jr., Regulation of innate antiviral defenses through a shared repressor domain in RIG-I and LGP2, Proc. Natl. Acad. Sci. U. S. A. 104 (2) (2007) 582–587.
[42] K. Honda, T. Taniguchi, IRFs: master regulators of signalling by Toll-like receptors and cytosolic pattern-recognition receptors, Nat. Rev. Immunol. 6 (9) (2006) 644–658.
[43] T. Kawai, S. Akira, The role of pattern-recognition receptors in innate immunity: update on Toll-like receptors, Nat. Immunol. 11 (5) (2010) 373–384.
[44] Y.M. Loo, M. Gale Jr., Immune signaling by RIG-I-like receptors, Immunity 34 (5) (2011) 680–692.
[45] H.J. Ramos, M. Gale Jr., RIG-I like receptors and their signaling crosstalk in the regulation of antiviral immunity, Curr Opin Virol 1 (3) (2011) 167–176.
[46] K.M. Quicke, K.Y. Kim, C.M. Horvath, M.S. Suthar, RNA helicase LGP2 negatively regulates RIG-I signaling by preventing TRIM25-mediated caspase activation and recruitment domain ubiquitination, J. Interferon Cytokine Res. 39 (11) (2019) 669–683.
[47] S. Rothenfusser, N. Goutagny, G. DiPerna, M. Gong, B.G. Monks, A. Schoenemeyer, M. Yamamoto, S. Akira, K.A. Fitzgerald, The RNA helicase Lgp2 inhibits TLR-independent sensing of viral replication by retinoic acid-inducible gene-I, J. Immunol. 175 (8) (2005) 5260–5268.
[48] A.M. Bruns, G.P. Leser, R.A. Lamb, C.M. Horvath, The innate immune sensor LGP2 activates antiviral signaling by regulating MDA5-RNA interaction and filament assembly, Mol. Cell 55 (5) (2014) 771–781.
[49] S.N. Chen, P.F. Zou, P. Nie, Retinoic acid-inducible gene I (RIG-I)-like receptors (RLRs) in fish: current knowledge and future perspectives, Immunology 151 (1) (2017) 16–25.
[50] J. Liu, J. Li, J. Xiao, H. Chen, L. Lu, X. Wang, Y. Tian, H. Feng, The antiviral signaling mediated by black carp MDA5 is positively regulated by LGP2, Fish Shellfish Immunol. 66 (2017) 360–371.
[51] W. Chen, C. Han, B. Xie, X. Hu, Q. Yu, L. Shi, Q. Wang, D. Li, J. Wang, P. Zheng, Y. Liu, X. Cao, Induction of Siglec-G by RNA viruses inhibits the innate immune response by promoting RIG-I degradation, Cell 152 (3) (2013) 467–478.